Electronic Supplementary Material (ESI) for ChemComm.

Design and Applications of Water Irradiation Devoid RF Pulses for Ultra-High Field Biomolecular NMR Spectroscopy

V. S. Manu[a], Cristina Olivieri[a], KowsalyaDevi Pavuluri[b], and Gianluigi Veglia*[a,c]

[a] *Department of Biochemistry, Molecular Biology & Biophysics, University of Minnesota, 312 Church St. SE, Minneapolis, MN 55455, USA*
[b] *Department of Radiology Mayo Clinic, Rochester, MN 55905*
[c] *Department of Chemistry, University of Minnesota, Minneapolis, MN 55455*

Table of contents

NMR Sample preparation

Three different proteins were analyzed: U-^{15}N-labeled K48C Ubiquitin mutant (Ubi^{K48C}), U-^{2}H, ^{15}N, ^{13}CH^{3} ILV-labeled C subunit of protein kinase A (PKA-C), and U-^{13}C-^{15}N labeled maltose binding protein (MBP). Briefly, recombinant U-^{15}N-labeled Ubi^{K48C} was expressed in *E. coli* BL21 (DE3) cell at 30 °C and purified as described previously.[1] Lyophilized ^{15}N-Ubi^{K48C} powder was resuspended in 10 mM sodium acetate buffer (pH 6.0) with 100 mM NaN_3 to a final concentration of 0.5 mM. Murine U-^{2}H,^{15}N,$^{13}CH_3$ ILV-PKA-C was expressed and purified as reported previously.[2, 3] The most abound isoform of PKA-C (isoform II, with phosphorylation at S338, T197, and S10) was concentrated and resuspended to a final concentration of 0.25 mM in 20 mM KH_2PO_4 (pH 6.5), 10 mM DTT, 10 mM $MgCl_2$, and 1 mM NaN_3 buffer supplied with 12 mM ATPγN, 5% $^{2}H_2O$, and 0.5% Pefa block® (Sigma-Aldrich, USA). Recombinant U-^{13}C-^{15}N MBP was expressed as described for the standard protocol of NEBExpress®. Briefly, transformed *E. coli* BL21 DE3 cells were cultured in M9 minimal medium containing $^{15}NH_4Cl$ (CIL, USA) and ^{13}C-glucose (CIL, USA) as the only nitrogen and carbon sources, respectively. Protein expression was induced at OD_{600} of 0.8 using 1 mM of Isopropyl β- d-1-thiogalactopyranoside (IPTG), and the cells were grown at 30 °C and harvested after 5 hours. The cell pellet was resuspended in 20 mM phosphate buffer (PBS) at pH 7.3, 120 mM NaCl, 1 mM EDTA, mM 0.15 mg/mL lysozyme, 0.05% glycerol, 2 mM dithiothreitol (DTT), 1 tablet of protease inhibitor (cOmplete™, Roche Applied Science), and 100 U/mL DNAse I (Roche Applied Science). The cell resuspension was homogenized with a cell grinder and sonicated using Branson Sonifier 450 (output of 4; duty cycle, 40%) for 10 min. Cell debris was pelleted by centrifugation at 45,700 g for 20 min at 4°C, and the pooled supernatant containing MBP was incubated with amylose resin (NEB, USA) and stirred overnight at 4°C. The protein/resin suspension was added to a gravity column and washed with 20 mM PBS (pH 7.3), 120 mM NaCl, and 1 mM EDTA buffer. MBP was eluted with ~100 mL of 20 mM PBS (pH 7.3), 120 mM NaCl, 1 mM EDTA buffer containing 60 mM of maltose. To eliminate contaminants, the elution fraction was then concentrated and further purified using size exclusion chromatography (Superdex 200, GE Healthcare Life Sciences, USA). The mass of the purified MBP was assessed using mass spectrometry. The final sample consisted of 1 mM MBP in 10 mM Na_2HPO_4, 0.1 mM EDTA and 1 mM NaN_3 buffer.

NMR Experiments

All experiments were recorded using U-^{15}N labeled K48C mutant of ubiquitin on a Bruker 850 MHz spectrometer equipped with a TCI cryoprobe at 300 K. The 3-9-19 water suppression spectra were acquired using the *p3919gp* pulse program with an RF amplitude of 16.67 kHz and inter-pulse delay 200 ms (=2xD19). The excitation sculpting experiments were recorded using the *zgesgp* pulse program with 5 ms selective pulses (Sinc1.1000). The 1D WADE pulse sequence was implemented by replacing 3-9-19 pulses in the *p3919gp* pulse program with a WADE-π pulse as shown in Fig. S2B, with an RF amplitude of 5 kHz or 1.25 kHz. The 1D water presaturation was recorded using the *zgpr* sequence. All experiments were recorded with 16 scans and an inter-scan delay of 1 second. The receiver gain was set to 32 dB for all the experiments. All spectra were processed using the Bruker TopSpin® software, and the spectra were processed using an exponential line broadening of 1 Hz.

The spectra of U-^{2}H, ^{15}N, $^{13}CH_3$ ILV-labeled catalytic subunit of protein kinase A were acquired on a Bruker 850 MHz spectrometer at 300K. The number of scan and dummy scans were set to 32 and 64, respectively, with an interscan delay of 1.5 seconds. 64 complex FIDs were acquired in the indirect dimension with a maximum evolution time of 21.2 ms. All experiments were processed using the identical processing parameters. A linear prediction was applied on the indirect dimension using LPfc and NCOEF of 32. All the matrices were zero-filled to a final size of 4096 x 2048 points. The baseline correction in the direct dimension was performed using '*qpol*'. For the B_1 response study, the RF power of ^{1}H channel was scaled to match an amplitude change of ±15% in steps of ±5% from the optimal calibrated RF amplitude. For the sensitivity study, we integrated each selected peaks using the TopSpin® command *intser*.

The U-^{13}C-^{15}N labeled Maltose Binding Protein (MBP) spectra were acquired on a Bruker 900 MHz spectrometer equipped with a TCI cryoprobe at 298K. Four standard TROSY pulse sequences implemented in the Bruker library: trosyetf3gpsi.2, trosyetf3gpsi, trosyetf3gpsi2, and trosyf3gpphsi19.2 [4-11] were compared with the new WADE-TROSY pulse program using identical acquisition parameters. The number of scans and dummy scans were set to 8 and 32, respectively, with an inter-scan delay of 1.5 seconds. 256 complex FIDs were acquired in the indirect dimension with a maximum evolution time in the indirect dimension of 75 ms. All experiments were processed using identical parameters. All the matrices were zero-filled to a size of 2048 x 1024 points. The baseline correction in the direct dimension was performed using the *qpol* command. The calibrated RF amplitudes in ^{1}H and ^{15}N channels were 19.2 kHz and 7.8 kHz, respectively.

Simulations of the response curves

All the simulations of the response curves presented in this manuscript were carried out in Matlab® using in-house scripts. The offset and RF amplitude responses of the 3919, W5, and WADE-π (Figures S2, S4, and S5) were performed by simulating the sequence 'Gradient– Binomial Pulse – Gradient', whereas for PM1, PM2, and OS1JRS10 (Figure S4) we simulated the sequence' Gradient1– Binomial Pulse – Gradient1 – Gradient2– Binomial Pulse – Gradient2'. The initial state was set to Mx, and the portion of the Mx magnetization at the end of each sequence was calculated for different offset values. The gradients were calculated by averaging more than 1000 simulations of the pulse sequences at different frequencies.

Supplementary figures

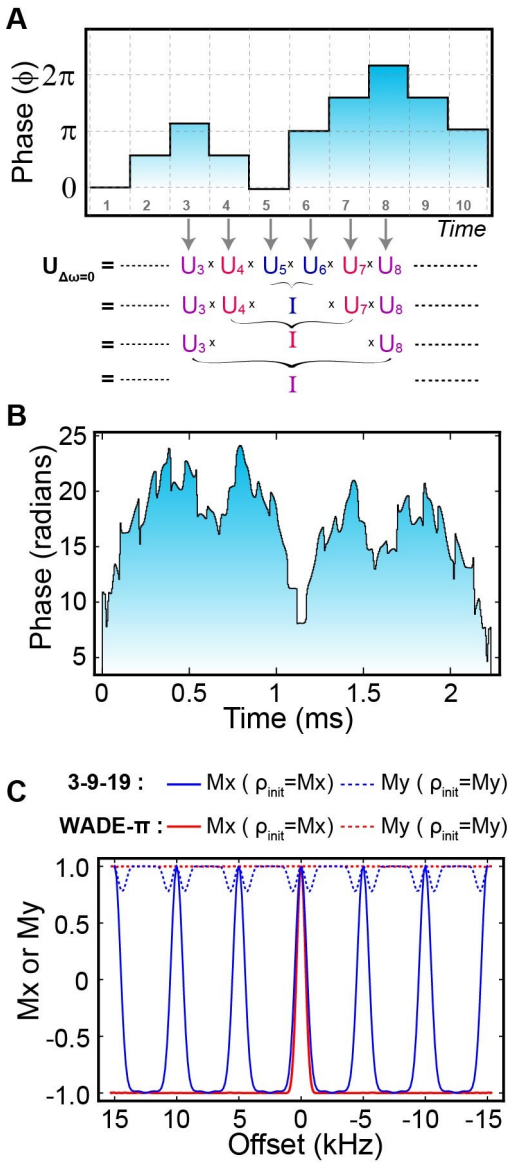

Figure S1. **Design of WADE-π pulses. A**. schematic representation of the p-shifted symmetry pulses used in WADE-π. **B**. Phase shape of the WADE-π pulse at a constant amplitude of 5 kHz. **C**. Performance of the refocusing operation obtained with WADE-π (red) and 3-9-19 (blue) pulses with the initial states M_x (solid) and M_y(dotted). The 3-9-19 pulse has an inter-pulse delay of 200 μs to match the water selectivity obtained with WADE-π. The RF amplitude of 3-9-19 pulse is 25 kHz.

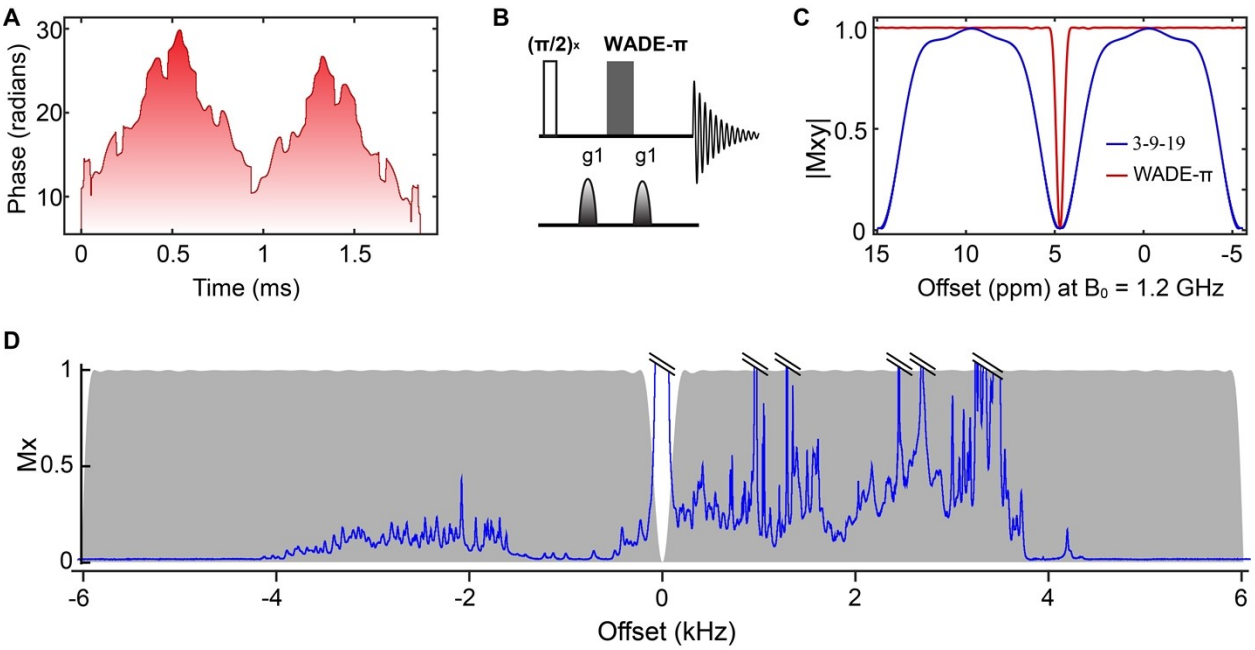

Figure S2. WADE-π pulse for water suppression at 1.2 GHz and offset response. A. Phase shape of WADE-π at a constant amplitude of 4.2 kHz. **B**. The 1D water suppression pulse sequence using WADE-π pulse. **C**. Simulated offset response of the transverse magnetization for the 1D water suppression pulse sequence. The WADE-π pulse response (red) shows the suppression of the water signal on-resonance with high selectivity. The inversion profile covers the entire bandwidth spanned by the amide proton resonances. The 3-9-19 water suppression response (blue) was simulated using B_1 = 25 kHz and an inter-pulse delay of 70 μs. **D.** Offset response of WADE- π pulse used in the 1D experiments along with experimental results with UBI^{K48C} in a Bruker 850 MHz spectrometer.

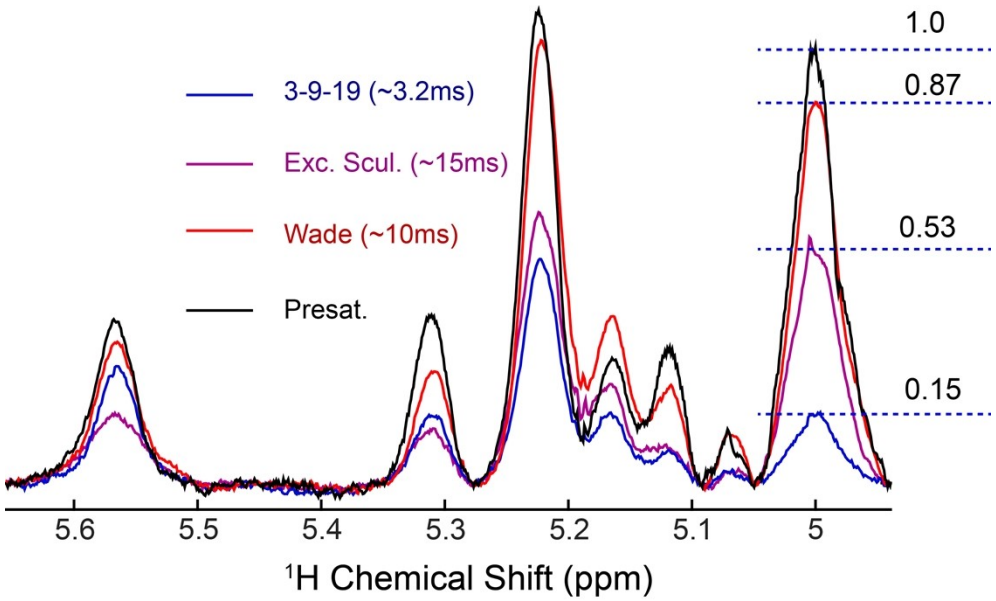

Figure S3. Portion of 1D ^{1}H spectra for different water suppression schemes. The presaturation sequence has the highest sensitivity for these non-exchanging peaks, whereas the 3-9-19 sequence has the lowest sensitivity. The reduction in sensitivity for WADE (0.87) and excitation sculpting (0.53) relative to the presaturation sequence is due to the longer duration of these water suppression schemes. All the spectra are normalized to the same noise level.

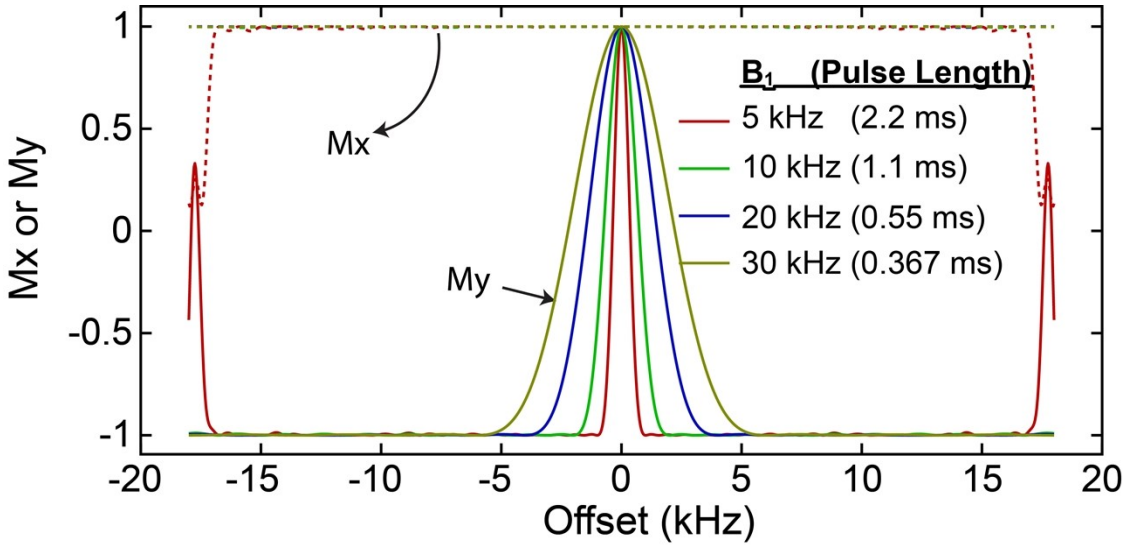

Figure S4. Tunability of the water suppression using WADE-π pulses. Offset response of WADE-π at different RF amplitudes (30, 20, 10, and 5 kHz) for M_x (dotted lines) and M_y (solid lines) magnetizations. The width of selectivity increases with the RF amplitude

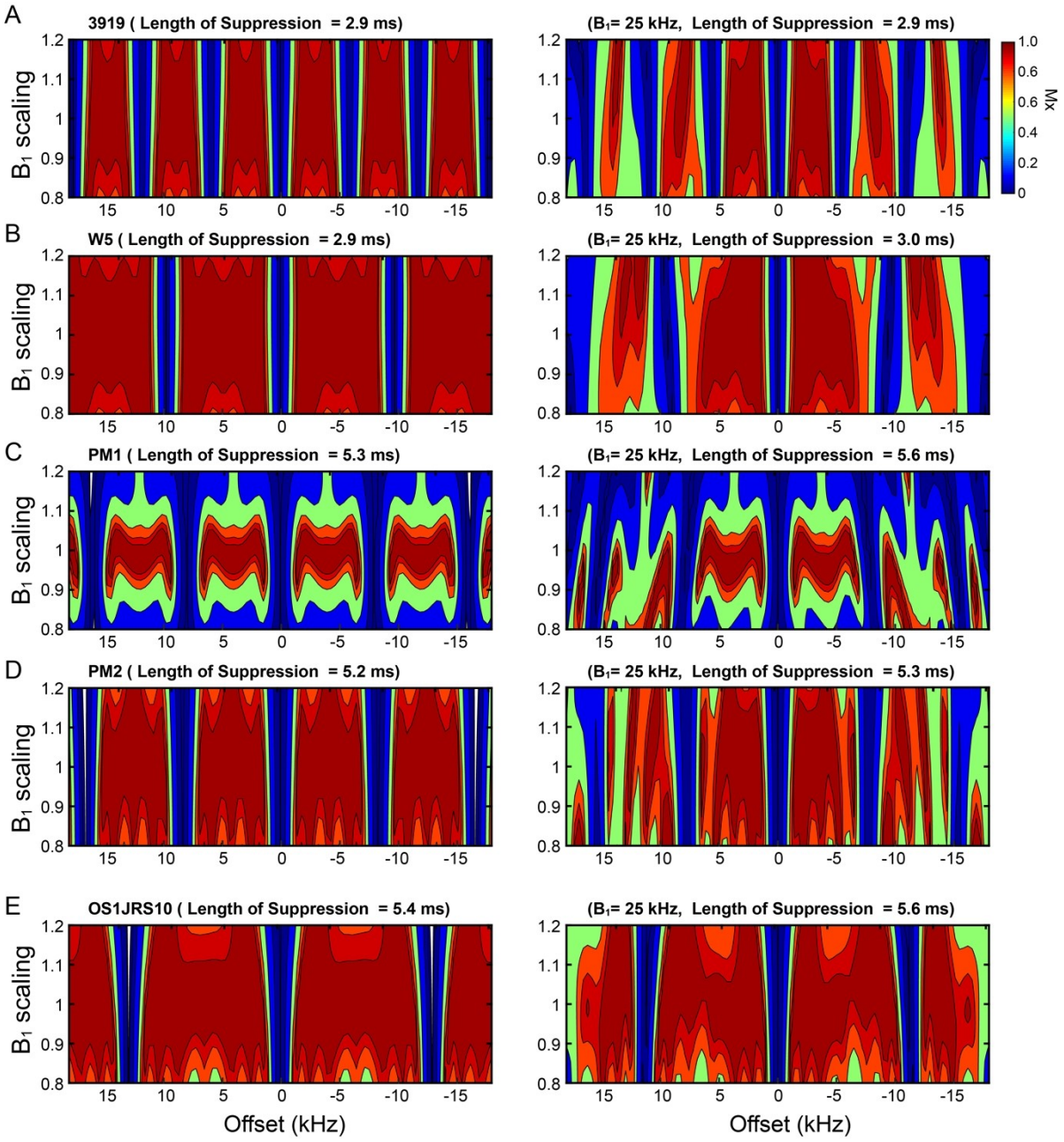

Figure S5. Comparison of the offset and RF amplitude (B_1) scaling response for the different binomial-like sequences used for water suppression. A 3-9-19[12], **B** W5[13], **C** PM1[14], **D** PM2[14], and **E** OS1 JRS10[15]. The response profiles were generated by simulating the '*Gradient Pulse : Binomial Pulse : Gradient Pulse*' sequence for the 3919 and W5 sequences. The PM1, PM2, and OS1JRS10 were implemented by repeating the WATERGATE sequence with different gradient strengths. The first column represents an ideal case without the effects of the finite pulse duration. The second column shows the simulated sequences with an RF amplitude of 25 kHz, considering the finite pulse duration. The length of suppression is the total time for executing the sequence, including the gradients pulses (1ms). The width of the identity operation on-resonance (i.e., width of the water selection) is kept constant in all the simulations (0.95 fidelity at 1.6 ppm away from on-resonance). The simulations are performed for a static magnetic field (B_0) of 900 MHz.

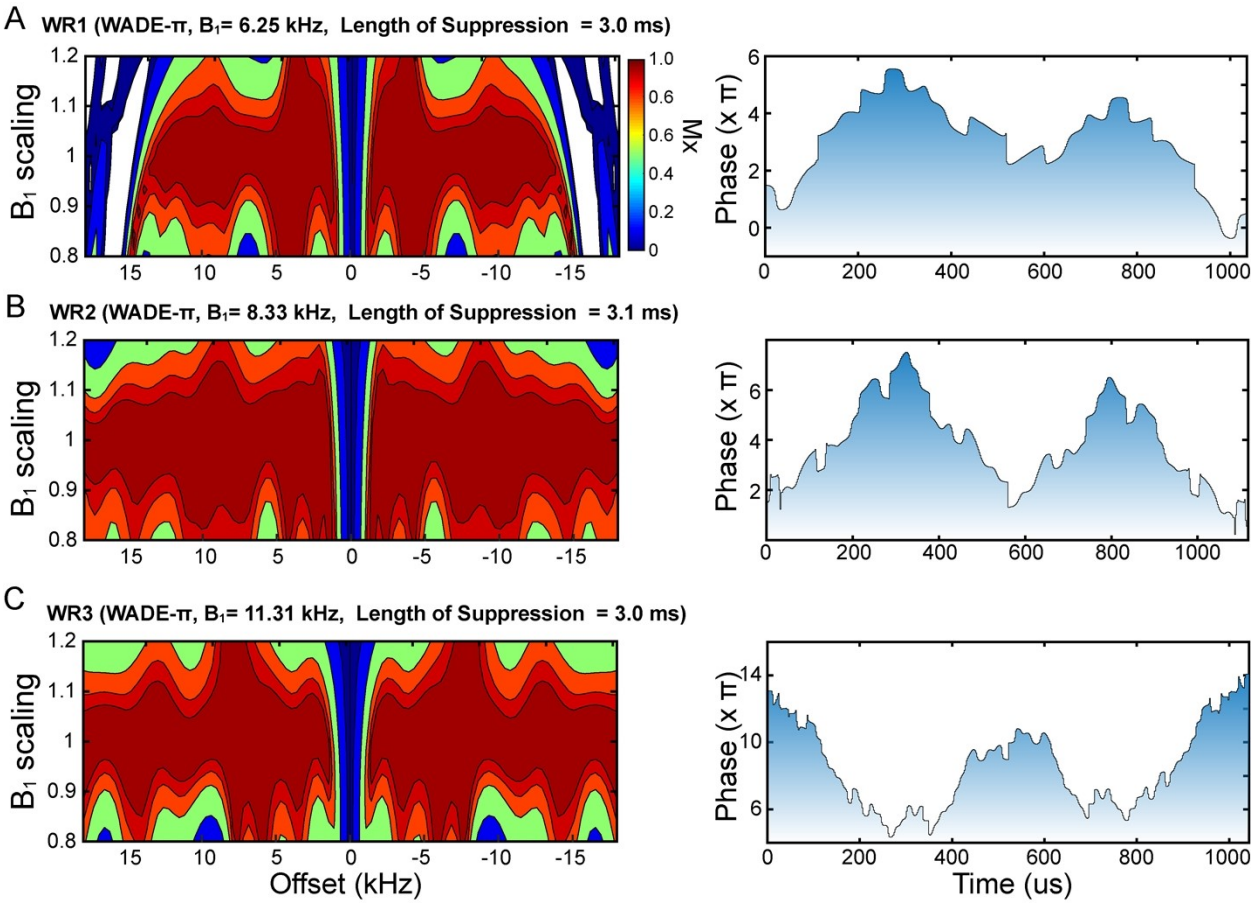

Figure S6. Offset and Amplitude response of different WADE-π pulses. A. WR1 with a bandwidth of 13.4 kHz and an RF amplitude of 6.25 kHz, **B**. WR2 with a bandwidth 26.8 kHz with an RF amplitude of 8.33 kHz, and **C**. WR3 with a bandwidth of 50 kHz with an RF amplitude of 11.31 kHz. All simulations were performed for a sequence 'Gradient Pulse: WADE-π: Gradient Pulse' for a 900 MHz spectrometer. The phase shapes of the WADE-π pulses are shown in the second column. The length of suppression is the total time for executing the sequence, including the gradients pulses (1ms). The width of water selection on-resonance is kept constant in all the simulations (0.95 fidelity at 1.6 ppm away from on-resonance).

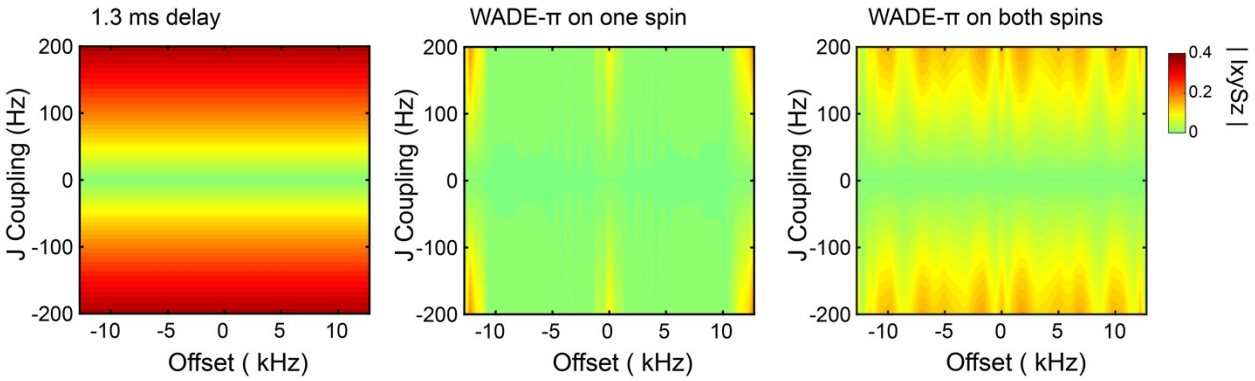

Figure S7. Simulations of the **J coupling response of the WADE-π pulses.** Response of 'J evolution' during the WR1 pulse of Figure S6A at different offset. Starting with an initial state of Ix, the effect of the J evolution is measured by the extent of IxSz / IySz operators created during the evolution of the pulse. (Left) J evolution for a delay equivalent to the WR1 pulse. (Middle) Response of WR1 applied on single spin. (Middle) Response of WR1 applied on both spins.

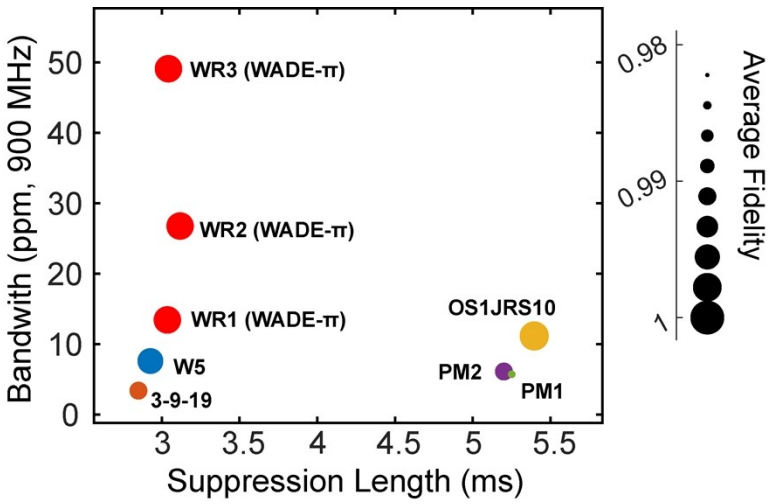

Figure S8. Bandwidth versus water suppression length for the binomial-like sequences calculated for the same water selectivity. The length of suppression includes the length of binomial pulses and the gradient pulses. The bandwidth is the region where operational fidelity is greater than 0.95 on either side of the on-resonance 'null' point. The size of each 'dot' represents the average fidelity within the bandwidth for each pulse. All simulations were performed for a static magnetic field (B_0) of 900 MHz.

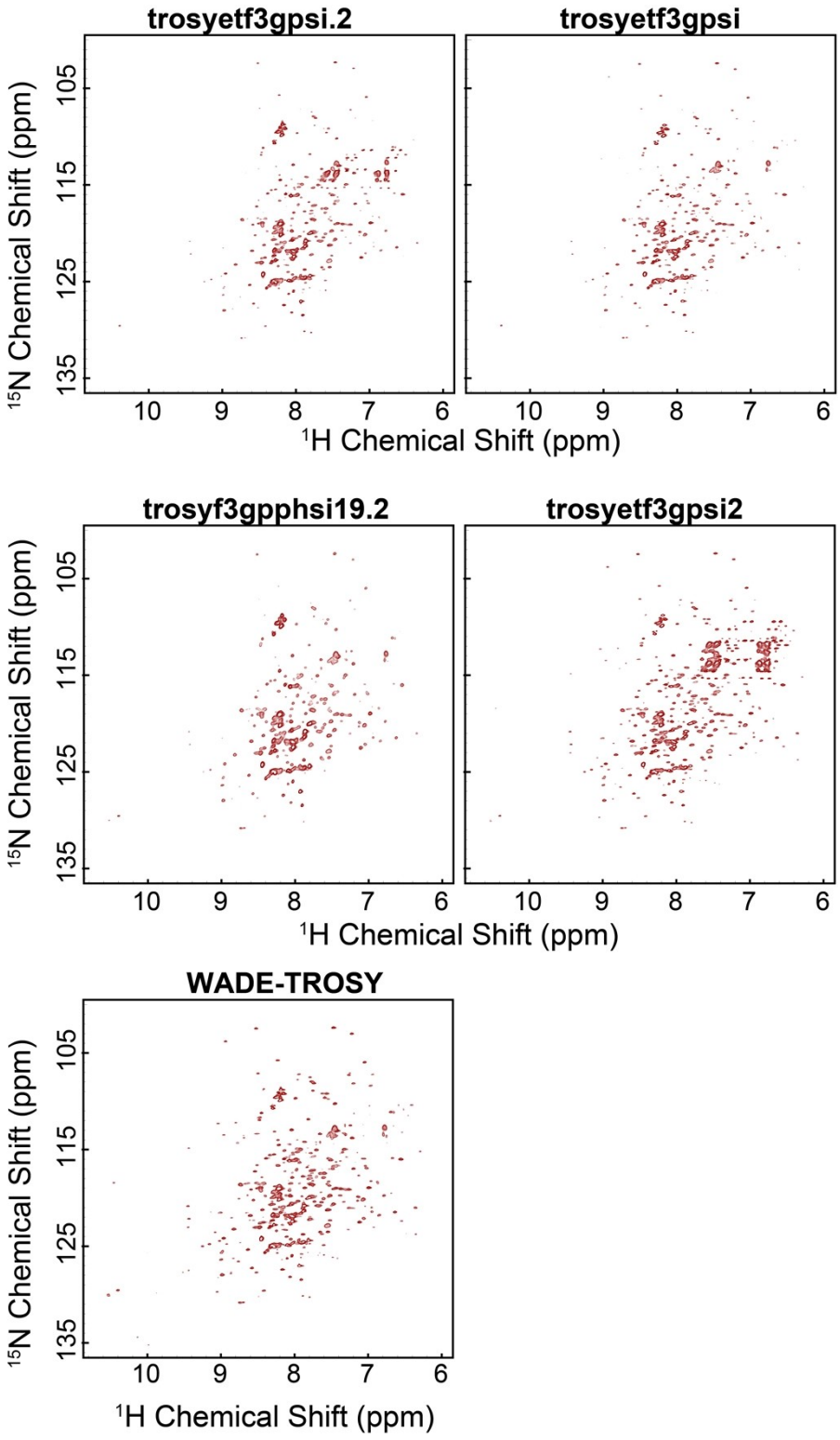

Figure S9. 2D TROSY-HSQC experiments recorded on U-^{13}C,^{15}N labeled MBP. The TROSY-HSQC spectra were acquired with pulse sequences from the Bruker Topspin library (*trosyetf3gpsi.2*, *trosyetf3gpsi*, *trosyetf3gpsi2*, and *trosyf3gpphsi19.2*) and are compared with the WADE-TROSY spectrum. All the spectra were recorded with 8 scans on a 900 MHz Bruker spectrometer and processed with identical parameters.

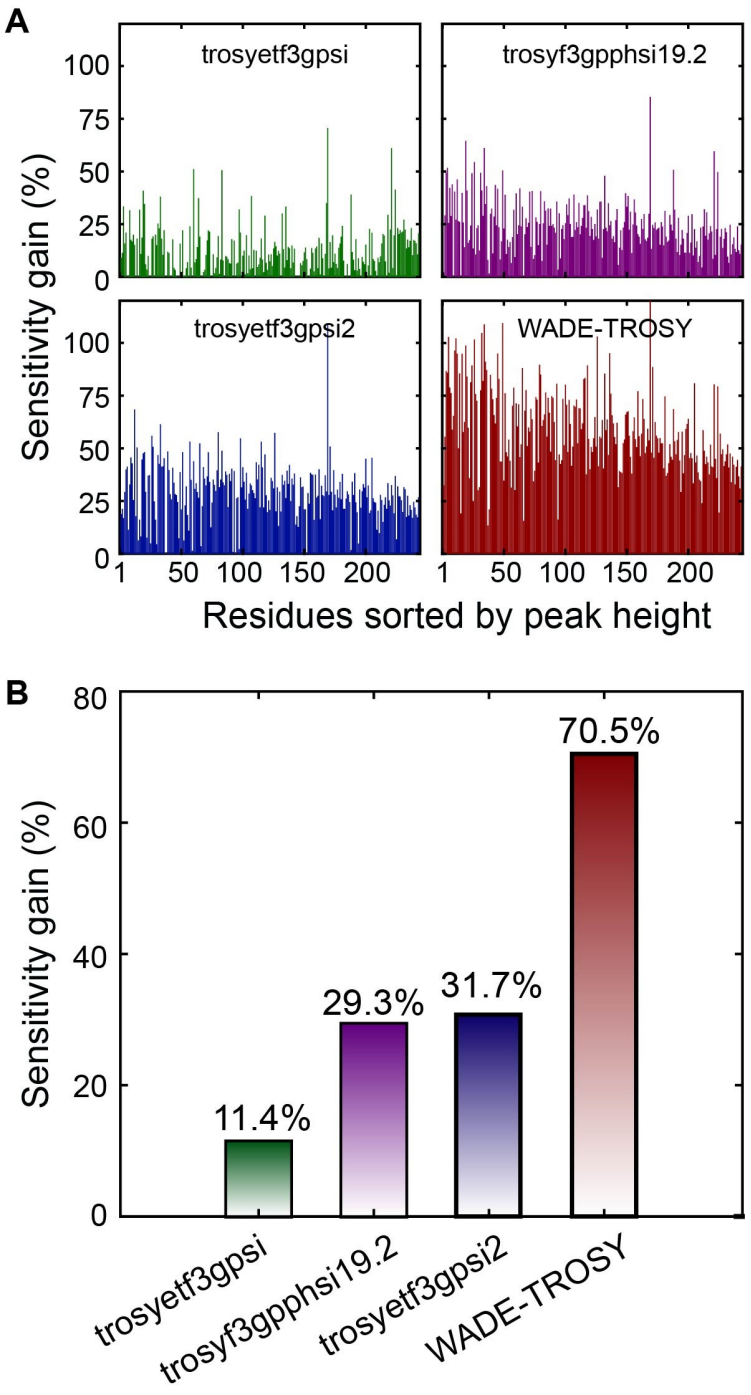

Figure S10. **Comparison of spectral sensitivity of the different TROSY-HSQC experiments recorded on U-^{13}C,^{15}N labeled MBP. A**. Gain in sensitivity of TROSY-HSQC correlation peaks for *trosyetf3gpsi* (green), *trosyetf3gpsi.2* (blue), *trosyf3gpphsi19.2* (purple), and WADE-TROSY (red). The resonances were randomly assigned and individually normalized with respect to the *trosyetf3gpsi.2* experiment, which is the least sensitive experiment. The peaks in the x axis were arranged in ascending order of intensity, with the least intense peaks are on the left side of the plot. **B**. Average sensitivity gain for the 50 least sensitive peaks evaluated for all TROSY-HSQC experiments. The WADE-TROSY-HSQC improves the sensitivity by ~70%, whereas the *trosyetf3gpsi2*, which is the most sensitive experiment in Bruker library is ~31%.

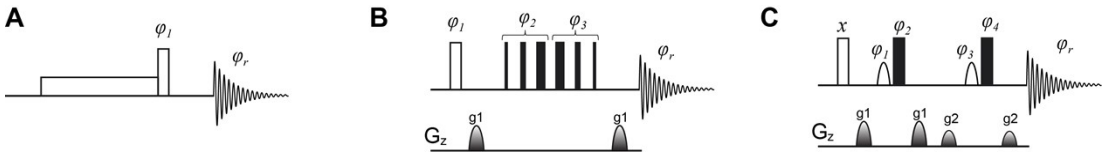

Figure S11. Pulse sequences used to acquire the 1D experiments reported in Figure 1. **A**. ^{1}H presaturation sequence,

Short Name	Full Name	Operation Type	Nuclei	Pulse Length factor	Amplitude (B_1)	Pulse Length	Bandwidth	Reference
WR0	wade_pix_44.017p1_bw6.72B1.mrf	WADE-π	^{1}H	44.017	5 kHz	44.017*50us = 2200.85us	6.72*B_1	Figure 1
WR1	wade_pix_25.900p1_bw4B1.mrf	WADE-π	^{1}H	25.9	5 kHz	25.9*50us = 1295us	4*B_1	Figure S6
WR2	wade_pix_37.250p1_bw6.08B1.mrf	WADE-π	^{1}H	37.25	5 kHz	37.25*50us = 1862.5us	6.08*B_1	Figure S6

where the long pulse represents the low-power saturation RF and short pulse is the π/2 reading pulse. The phase cycles for ϕ_1 and receiver phase(ϕ_r) are the same (x, -x, -x, x, y, -y, -y, y). **B**. 1D ^{1}H sequence with 3919 water suppression. The phase cycles are ϕ_1={x, -x}, ϕ_2={x, x, y, y, -x, -x, -y, -y}, ϕ_3={-x, -x, -y, -y, x, x, y, y} and ϕ_r={x, -x, -x, x}, **C**. 1D 1H sequence with excitation sculpting. The filled rectangles represent π hard pulses and the shaped pulses are water selective π pulses. The phase cycles are ϕ_1={x, y}, ϕ_2={-x, -y}, ϕ_3={ x, x, y, y}, ϕ_4={ -x, -x, -y, -y} and ϕ_r={x, -x, -x, x}.

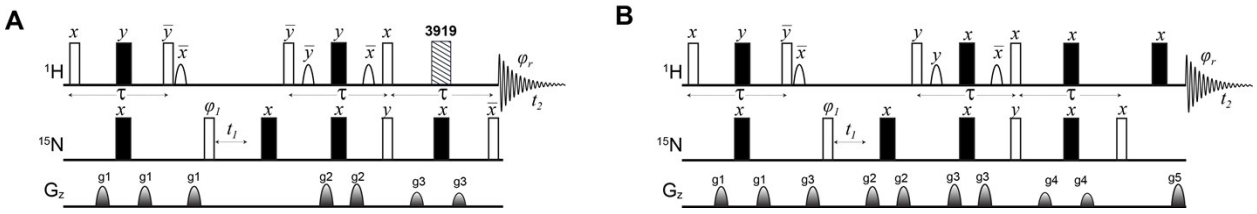

Figure S12. Modified [^{1}H-^{15}N] TROSY pulse sequences with flip-back pulses. A. *trosyf3gpphsi19.2* sequence with a 3919 water suppression. The phase cycles for ϕ_1 and receiver phase(ϕ_r) are y, -y, -x, x and x, -x, -y, y, respectively. The length of all gradient pulses is 1 ms and the ratios of the gradient strengths are 30:45:50 for g1:g2:g3. B. *trosyetf3gpsi* sequence. Gradient pulse length for g1, g3 and g4 is 1 ms. The pulse length for g2 and g5 is 600 μs. The ratios of gradient strengths are 30:80:45:50:16.2 for g1:g2:g3:g4:g5. The phase cycles for ϕ_1 and ϕ_r are y, -y, -x, x and x, -x, -y, y respectively. The open rectangles are π/2 pulses and filled rectangles are π pulses for inversion and refocusing operations. The shaped pulses in the ^{1}H channel are water flip-back pulses of 1 ms.

WR3	wade_pix_47.200p1_bw8B1.mrf	WADE-π	^{1}H	47.2	5 kHz	47.2*50us = 2360us	$8*B_1$	Figure S6
AR1	pix_7.984p1_bw0.70B1.mrf	Amide π	^{1}H	7.984	25 kHz	7.984*10us = 79.84us	$0.7*B_1$	Figure 2
IN1	z2iz_4.610p1_bw0.80B1.mrf	Inversion	^{15}N	4.610	7.1429 kHz	4.610*35us = 161.35us	$0.8*B_1$	Figure 2
UR1	pix_7.093p1_bw0.80B1.mrf	π	^{15}N	7.093	7.1429 kHz	7.093*35us = 248.255us	$0.8*B_1$	Figure 2
IN2	z2iz_10.021p1_bw2.40B1.mrf	Inversion	^{13}C	10.021	20.8333 kHz	10.021*12us = 12.252 us	$2.4*B_1$	Figure 2

Table S1. List of all the RF shapes used in this article. All the RF shapes are available at the University of Minnesota repository site https://hdl.handle.net/11299/228028 and to the GitHub https://github.com/manuvsub/WADE_TROSY_v1.0. The RF amplitude tuned for the required bandwidth.

Additional reference

1. C. Olivieri, M. V. Subrahmanian, Y. Xia, J. Kim, F. Porcelli and G. Veglia, *J Biomol NMR*, 2018, **70**, 133-140.
2. C. Olivieri, Y. Wang, G. C. Li, S. M. V, J. Kim, B. R. Stultz, M. Neibergall, F. Porcelli, J. M. Muretta, D. D. Thomas, J. Gao, D. K. Blumenthal, S. S. Taylor and G. Veglia, *Elife*, 2020, **9**.
3. J. Kim, Y. Wang, G. Li and G. Veglia, *Methods Enzymol*, 2016, **566**, 35-57.
4. A. Meissner, T. Schulte-HerbrÜGgen, J. Briand and O. W. SØRensen, *Molecular Physics*, 1998, **95**, 1137-1142.
5. J. Weigelt, *Journal of the American Chemical Society*, 1998, **120**, 12706-12706.
6. M. Czisch and R. Boelens, *J Magn Reson*, 1998, **134**, 158-160.
7. K. Pervushin, R. Riek, G. Wider and K. Wüthrich, *Proceedings of the National Academy of Sciences*, 1997, **94**, 12366-12371.
8. G. Zhu, X. M. Kong and K. H. Sze, *J Biomol NMR*, 1999, **13**, 77-81.
9. D. Nietlispach, *J Biomol NMR*, 2005, **31**, 161-166.
10. T. Schulte-Herbruggen and O. W. Sorensen, *J Magn Reson*, 2000, **144**, 123-128.
11. M. Rance, J. P. Loria and A. G. r. Palmer, *J Magn Reson*, 1999, **136**, 92-101.
12. V. Sklenar, M. Piotto, R. Leppik and V. Saudek, *Journal of Magnetic Resonance, Series A*, 1993, **102**, 241-245.
13. M. Liu, X.-a. Mao, C. Ye, H. Huang, J. K. Nicholson and J. C. Lindon, *Journal of Magnetic Resonance*, 1998, **132**, 125-129.
14. G. Zheng, A. M. Torres and W. S. Price, *Journal of Magnetic Resonance*, 2008, **194**, 108-114.
15. T. Brenner, J. Chen, T. Stait-Gardner, G. Zheng, S. Matsukawa and W. S. Price, *Journal of Magnetic Resonance*, 2018, **288**, 100-108.